



Modeling The Microrelief Structure of Ti6Al4V Titanium Alloy Surface After Exposure to Femtosecond Laser Pulses

Iaroslav Lytvynenko¹, Pavlo Maruschak^{1*}, Hermann Seitz², Georg Schnell²

¹Ternopil Ivan Puluj National Technical University, 56, Ruska str., 46001 Ternopil, UKRAINE

²Microfluidics, Faculty of Mechanical Engineering and Marine Technology, University of Rostock, Justus-von-Liebig-Weg 6, 18059 Rostock, GERMANY

*Corresponding Author

DOI: <https://doi.org/10.30880/ijie.2022.14.04.008>

Received 28 September 2020; Accepted 13 December 2021; Available online 20 June 2022

Abstract: A method of mathematical modeling of the ordered surface relief of titanium alloy Ti6Al4V after femtosecond laser treatment is proposed, which allowed obtaining the informative signs of the self-organized surface irregularities, taking into account the stochastic and cyclic nature of this process. An algorithm has been developed, and a package of computer programs has been created based on the proposed mathematical model. These methods make it possible to analyze the zone-spatial two-dimensional structure of the cyclic relief of the modified surface. They are also the basis for creating the specialized software for the automated profilometric diagnostic systems.

Keywords: laser, microrelief, surface engineering, titanium alloys, topography.

1. Introduction

The size and shape of the implant microrelief are known to affect the process of osseointegration in bone tissue [1]. An effective tool for altering surface topography is the femtosecond laser treatment, which has already been shown in various studies. An effective tool for altering surface topography is the femtosecond laser treatment, which has already been shown in various studies [2, 3]. Particular attention is paid to optimizing the surface properties, increasing the specific surface area of the implant that comes into contact with bone tissue [4, 5]. This increases the rate of osseointegration, reduces stresses in the bone sections around the implant, and creates preconditions for optimizing the microgeometry of their surface. Such optimization is possible when conditions are created for its complete and accurate mathematical description [6, 7].

Mathematical models of implant surfaces allow making a quantitative comparison of the laser treatment efficiency, evaluating the geometric features of the relief, calculating the contact stresses in the zone of osseointegration, etc. A significant number of surface models are known, which take into account surface microgeometry. However, it should be borne in mind that a complete description of the properties of surface microgeometry requires from 3 to 25 parameters, which significantly complicates the process of optimizing surface properties [8-10]. Another important aspect is the ability to estimate the stress concentration in the surface microrelief and to conduct a rapid assessment of the impact of laser treatment on the residual cyclic durability.

Contemporary methods of profilometry make it possible to conduct functional diagnostics of the surface condition and reveal the ordered structural formations. However, it remains important to create effective computer diagnostic systems that perform automated processing of the profilometry signals obtained, which would allow for the analysis of surface microgeometry, followed by a preliminary diagnostic conclusion about its condition. The development of approaches to modeling the material surface condition is the basis for creating a new method of strengthening structural materials, modifying their surface [11-13].

*Corresponding author: vr.science.tntu@gmail.com

The objective of this research is to use a mathematical model of a cyclic random process for the surface relief morphology of titanium alloy Ti6Al4V exposed to femtosecond laser pulses, taking into account its stochastic and cyclic nature.

2. Research technique

A model for creating relief formations on the surface of titanium alloy Ti6Al4V, which were polished to a roughness $s = 0.065 \pm 0.003 \mu\text{m}$ and treated with a laser, is considered in this article. A 300 fs UFFL_60_200_1030_SHG fiber laser (Active Fiber Systems GmbH, Jena, Germany) featuring an amorphous glass Yb-doped core was used for laser structuring. The laser system is integrated into a Microgantry GU4 five-axis micromachining center (Kugler GmbH, Salem, Germany). The pulse repetition rate of the laser system can be varied from 50.3 kHz to 18.6 MHz, with an average power of up to 60W. The laser emits linear polarized light with a wavelength of 1030 nm. An f -theta lens with a focal length of 163 mm leads to a circular focus diameter of $d_f = 36$ microns at $1/e^2$ intensity (Gaussian laser beam profile). This spot diameter is used for all laser parameter calculations. The findings presented in article [14], in which pulse treatment was performed by overlapping the areas of laser treatment (LO), were the experimental basis of this research. High values of the parameters considered caused phase transformations and heat accumulation, which led to a reduced ablation threshold and increased roughness. In this paper, the surface relief properties of titanium alloy Ti6Al4V were modeled by LO 40% at a laser fluence of $q = 4.91 \text{ J/cm}^2$ to verify the method efficiency. A generalized theoretical and methodological approach, which consists in identifying the segmental structure of cyclic signals with a variable rhythm, was applied to the analysis of the surface relief, allowing us to process experimental data as part of the stochastic approach.

2.1. Mathematical model of the surface microrelief structure of the titanium alloy exposed to femtosecond laser pulses.

The profile diagram of the surface microrelief of titanium alloy Ti6Al4V after exposure to femtosecond laser pulses was considered as a stochastic cyclic signal. In [15], a cyclic random process is defined as a separable random process $\xi(\omega, l), \omega \in \Omega, l \in [0, L)$, which is called a cyclic random process of a continuous argument in the presence of function $T(l, n)$ that satisfies the conditions of the rhythm function [15]. In particular, finite-dimensional vectors $(\xi(\omega, l_1), \xi(\omega, l_2), \dots, \xi(\omega, l_k))$ and $(\xi(\omega, l_1 + T(l_1, n)), \xi(\omega, l_2 + T(l_2, n)), \dots, \xi(\omega, l_k + T(l_k, n)))$, $n \in \mathbf{Z}$, де $\{l_1, l_2, \dots, l_k\}$ is the set of the process separability $\xi(\omega, l), \omega \in \Omega, l \in [0, L)$ for all integers $k \in \mathbf{N}$, are stochastically equivalent in a broad sense. Parameter $T(l, n)$ is the rhythm function of the cyclic process, which reflects the variation of temporal (spatial, in our case) intervals between its single-phase values. The main properties of this function are described in [15].

Since the rhythm function $T(l, n)$ is taken into account in the model, it must meet the following requirements:

1. Function $T(l, n)$ is set throughout the whole real axis $l \in \mathbf{R}$ and the whole set of integers, and is equal to zero when $n = 0$. In other cases, it is either positive or negative, that is:

- a) $T(l, n) > 0$, if $n > 0$;
 - b) $T(l, n) = 0$, if $n = 0$;
 - c) $T(l, n) < 0$, if $n < 0$.
- (1)

2. Under any $l_1 \in \mathbf{R}$ or $l_2 \in \mathbf{R}$, for which $l_2 > l_1$, the following inequation is fulfilled for function $T(l, n)$:

$$l_1 + T(l_1, n) < l_2 + T(l_2, n), \forall n \in \mathbf{Z}. \tag{2}$$

If the rhythm function's conditions are fulfilled for the cyclic process investigated, which is repeated while unfolding in space (its statistical characteristics are repeated), then it is appropriate to apply the proposed mathematical model in the form of a cyclic random process.

This mathematical model has advantages, because the process stochasticity and cyclicity (as well as periodicity as a partial case) are taken into account, along with the variable rhythm of its deployment (or stable (constant) rhythm as a partial case (periodic rhythm)).

According to this mathematical model, the processing of cyclic microrelief was possible in the presence of its rhythm function, or subject to its finding. To do this, the segmental cyclic structure of the microrelief was taken into account as follows:

$$\xi_\omega(l) = \sum_{i=1}^C f_i(l), l \in \mathbf{W} \tag{3}$$

where C is the number of segments-cycles of the cyclic microrelief. W is the definition area of cyclic microrelief, while the definition area of its values in case of the stochastic approach is the Hilbert space of random variables given on one probabilistic space $(\xi_\omega(l) \in \Psi = L_2(\Omega, P))$. Within structure (3), the segments-cycles of the cyclic microrelief process were determined through indicator functions, that is

$$f_i(l) = \xi_\omega(l) \cdot I_{W_i}(l), i = \overline{1, C}, l \in W. \tag{4}$$

The indicator functions, which allocate segments-cycles, were defined as:

$$I_{W_i}(l) = \begin{cases} 1, l \in W_i, \\ 0, l \notin W_i. \end{cases} \tag{5}$$

where W_i is the definition area of the indicator function, which in the case of a discrete signal ($W=D$) is equal to a discrete set of signal sections

$$W_i = \{l_{i,j}, j = \overline{1, J}\}, i = \overline{1, C}, \tag{6}$$

The segmental cyclic structure is taken into account as a set of spatial sections

$$\{l_i\} \text{ or } \{l_{i,j}\}, i = \overline{1, C}, j = \overline{1, J} \tag{7}$$

Such expression of mathematical model (1) takes into account the rhythm of the cyclic microrelief through the continuous rhythm function $T(l, n)$, namely,

$$I_{W_i}(l) = I_{W_{i+n}}(l + T(l, n)), i = \overline{1, C}, n \in Z, l \in W. \tag{8}$$

To evaluate rhythm function $T(l, n)$, the segmental structure of microrelief (in our case, the segmental cyclic structure) was determined first as $\hat{D}_c = \{l_i, i = \overline{1, C}\}$, which is a set of spatial moments that correspond to the boundaries of segments-cycles of the microrelief.

2.2. Defining segmental cyclic structure of microrelief (evaluating segmental structure)

Given the well-founded mathematical model, the problem of segmenting cyclic microrelief with a segmental cyclic structure consisted in finding an unknown set of spatial moments of the boundaries of i -th segments-cycles $\hat{D}_c = \{l_i, i = \overline{1, C}\}$, which is similar to finding the division $W_i^c = \{W_i, i = \overline{1, C}\}$ of the cyclic microrelief definition area. In this case, it is necessary that for a certain set of spatial moments $\hat{D}_c = \{l_i, i = \overline{1, C}\}$, the bijection conditions of the microrelief cycles are met, and their strict ordering is observed, that is, isomorphism with respect to the order of microrelief sections (7), which correspond to segments-cycles with equal attributes (8), therefore:

$$l_i \leftrightarrow l_{i+1}, \dots; l_{i+1} > l_i, l \in W, i = \overline{1, C}, \tag{9}$$

$$p(f(l_i)) = p(f(l_{i+1})) \rightarrow A, l \in W, i = \overline{1, C}. \tag{10}$$

where A is the set of possible values of attributes.

Similar problems in digital cyclic data processing systems are solved in the analysis of ordered signals, in particular, cardio signals, cyclic signals of relief formations [16, 17], economic cycles, solar activity cycles, etc., whose mathematical models are represented by cyclic random processes. To do this, different methods can be used to solve the segmentation problem [18-22], but they must be, above all, consistent with the mathematical model that describes the self-organization of the process (physical phenomenon) in the relevant subject area. In this paper, the segmentation method presented in [23] is used. It allowed us to determine the segmental cyclic structure $\hat{D}_c = \{l_i, i = \overline{1, C}\}$ and its parameter. The structural diagram of the developed segmentation method is shown in Fig. 1. The results of applying the developed method of segmentation to the analyzed microrelief are shown in Fig. 2. Having obtained a segmental cyclic structure for estimating the continuous rhythm function of the microrelief, we determined its rhythmic structure (discrete rhythm function). Using this approach makes it possible to evaluate the properties of microrelief, which is important in technical diagnostics. In particular, it allows taking into account the geometry of protrusions on the self-organized surface, establishing their relationship with osseointegration.

2.3. Determining rhythmic cyclic structure of the microrelief (evaluating the rhythmicity of the structure)

A discrete rhythmic structure in case of a segmental cyclic structure of microrelief (see Fig. 3), with $W=D$, was determined as follows

$$\hat{T}(l_i, n) = l_{i+n} - l_i, i = \overline{1, C}, n \in Z. \tag{11}$$

Having obtained a rhythmic structure, we evaluated it taking into account the recommendations developed in [16, 24]. The evaluation of continuous rhythm function is described in [14]. An interpolation function $\hat{T}(l, n), l \in W, n \in Z$ was determined that would pass through discrete values of the rhythmic structure (discrete rhythm function) $\hat{T}(l_i, n), l_i \in W, i = \overline{1, C}, n \in Z$ and satisfy the conditions of the rhythm function $T(l, n)$. In particular, its derivative by argument l (in our case), if any, should not be less than minus one [16].

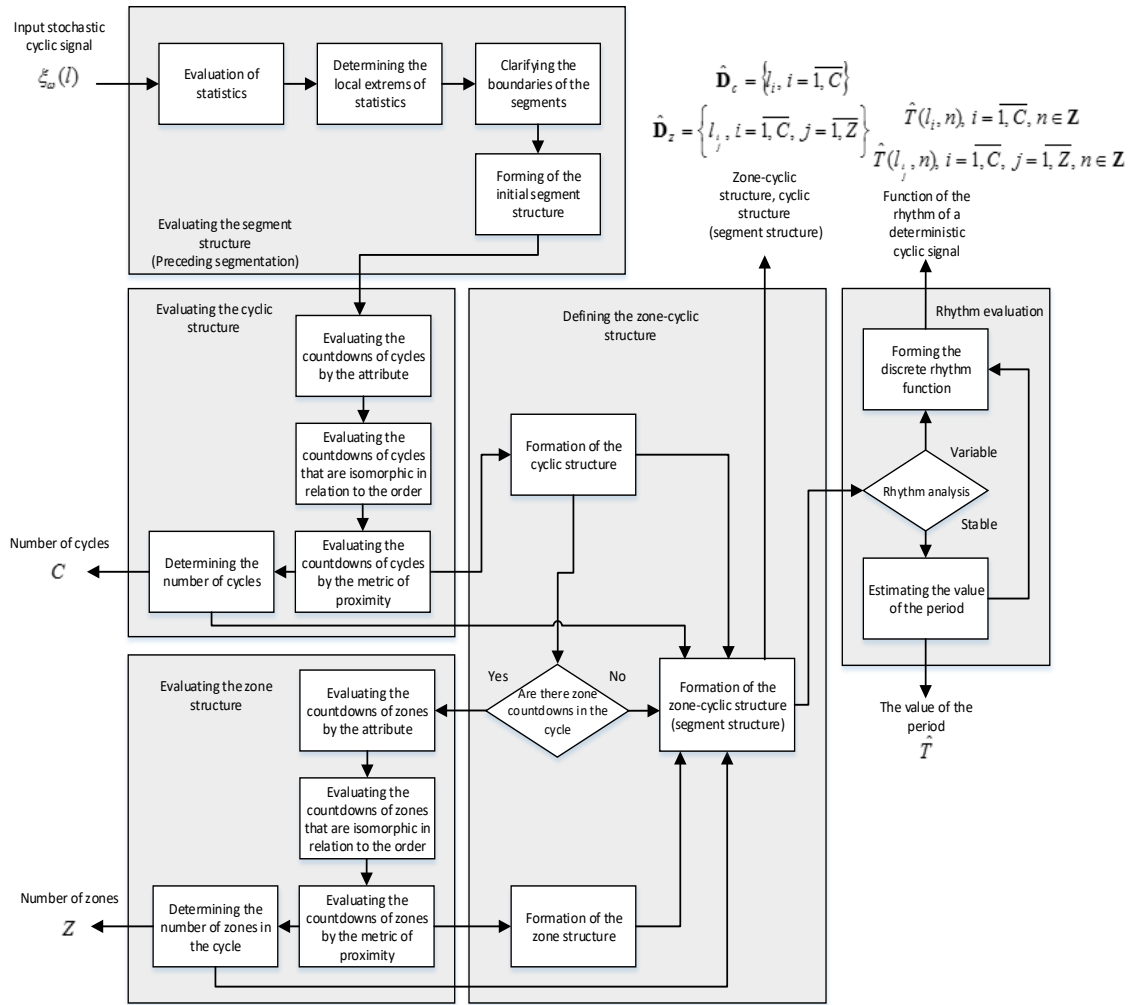


Fig. 1 - Algorithmic support for the method of segmentation of stochastic cyclic signals

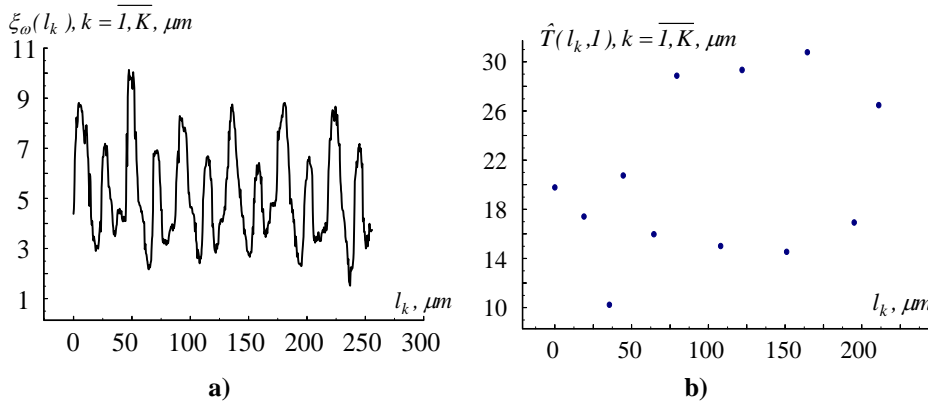


Fig. 2 - Description of the surface morphology of titanium alloy Ti6Al4V after exposure to femtosecond laser pulses as a cyclic process and its defined rhythmic structure: a) microrelief with LO 40%; b) discrete rhythmic cyclic structure of the microrelief section that corresponds to the boundaries of segments-cycles (determined by the segmentation method), calculated by formula (11)

In the practical application of diagnostic systems, they take into account the fact that the cyclic signal can only be processed when the rhythmic structure is determined, provided that $n > 0$. More precisely, they assume that $n = 1$ and perform statistical signal processing by means of sequential processing of cycles (the first, third, fifth cycle, and so on), but not individual cycles with a certain step, which is the case when $n = 2$. Therefore, we analyzed the rhythmic structures assuming that $n = 1$.

Continuous rhythm functions are evaluated using various approaches, including piecewise-linear interpolation, quadratic or cubic spline interpolation. In this work, we used the well-known method of piecewise linear interpolation [16]. The structural diagram of the method for estimating the rhythm function is shown in Fig. 3.

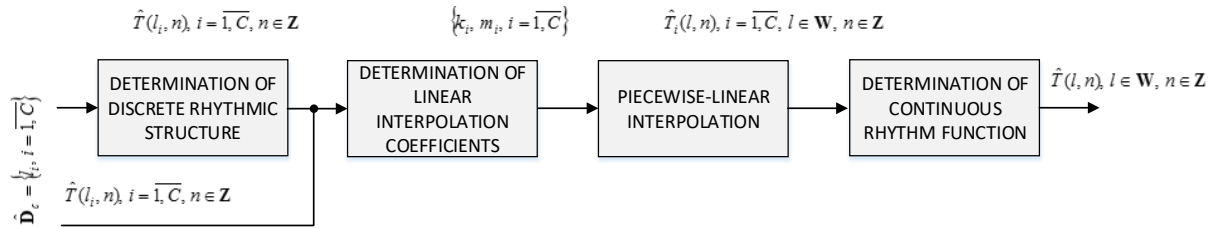


Fig. 3 - Structural diagram of the method for estimating the rhythm function of the cyclic microrelief of the surface of titanium alloy Ti6Al4V after exposure to femtosecond laser pulses by the method of piecewise linear interpolation

Piecewise linear interpolation was used to estimate the continuous rhythm function

$$\hat{T}_i(l, l) = k_i \cdot l + m_i, i = \overline{1, C}, l \in \mathbf{W} . \tag{12}$$

Interpolant coefficients were determined by the formulae:

$$k_i = \frac{\hat{T}(l_{i+1}, l) - \hat{T}(l_i, l)}{l_{i+1} - l_i}, i = \overline{1, C}, l_i \in \mathbf{W}, \tag{13}$$

$$m_i = \hat{T}(l_i, l) - \frac{\hat{T}(l_{i+1}, l) - \hat{T}(l_i, l)}{l_{i+1} - l_i} \cdot l_{i+1}, i = \overline{1, C}, l_i \in \mathbf{W}.$$

Rhythm function was estimated by the following formula

$$\hat{T}(l, l) = \sum_{i=1}^C \hat{T}_i(l, l), l \in \mathbf{W} . \tag{14}$$

An example of the evaluation of the continuous rhythm function is given in Fig. 4.

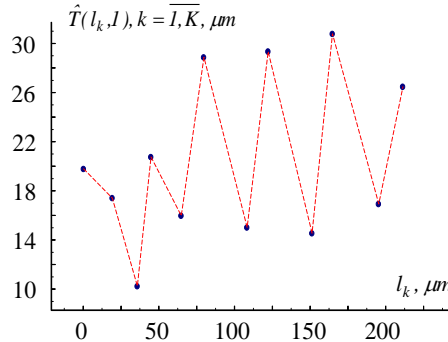


Fig. 4 - Rhythm function based on piecewise linear interpolation

3. Result and discussion.

Taking into account the mathematical model, we apply the developed methods of statistical processing presented in [25-28]. Statistical evaluation of the probabilistic characteristics of the cyclic random process (microrelief process) was performed taking into account the obtained rhythm function as follows:

- statistical evaluation of the mathematical expectation of the microrelief process was calculated as

$$\hat{m}_\xi(l_j) = \frac{1}{C} \cdot \sum_{j=0}^{C-1} \xi_\omega(l_j + T(l_j, n)), l_j \in \mathbf{W}_1 = [\tilde{l}_1, \tilde{l}_2). \tag{15}$$

- statistical assessment of the variance of the microrelief process

$$\hat{d}_\xi(l_j) = \frac{1}{C-1} \cdot \sum_{j=0}^{C-1} (\xi_\omega(l_j + T(l_j, n)) - \hat{m}_\xi(l_j + T(l_j, n)))^2, l_j \in \mathbf{W}_1 = [\tilde{l}_1, \tilde{l}_2). \tag{16}$$

where \tilde{l}_1, \tilde{l}_2 are the boundaries of the first cycle of cyclic microrelief.

In [24], other probability characteristics are defined, in particular, the correlation and covariance functions. We limited ourselves to these two characteristics because they are necessary for the next steps of modeling the microrelief morphology.

The results of the statistical estimates obtained are shown in Figure 5.

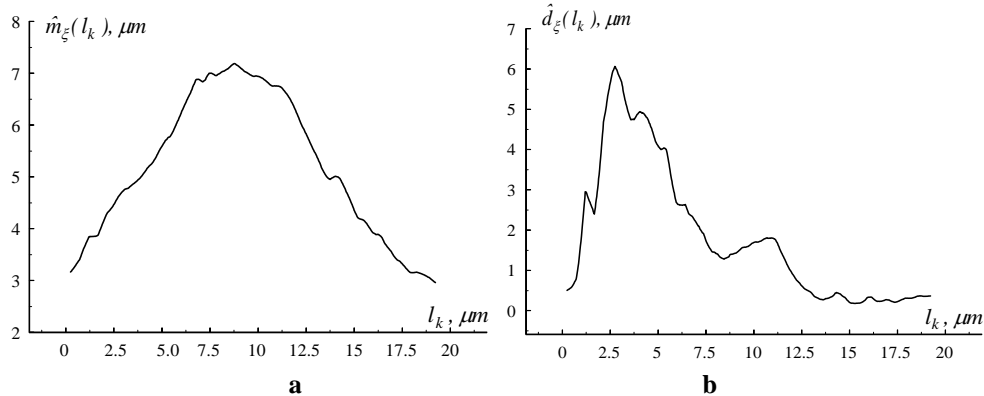


Fig. 5 - Statistical estimates of the microrelief cycles morphology of the surface of titanium alloy Ti6Al4V after exposure to femtosecond laser pulses: a) statistical evaluation of the mathematical expectation; b) statistical estimation of variance

The results of applying computer simulation experiments are shown in Figure 7. From the obtained results it was revealed that the simulated elements of the surface microrelief are close to the experimental ones, which indicates sufficient accuracy of statistical processing of cyclic signals. The mathematical model of forming a self-organized relief on the metal surface under the action of laser pulses as a cyclic random process is used in this research, and the methods of its statistical processing are substantiated.

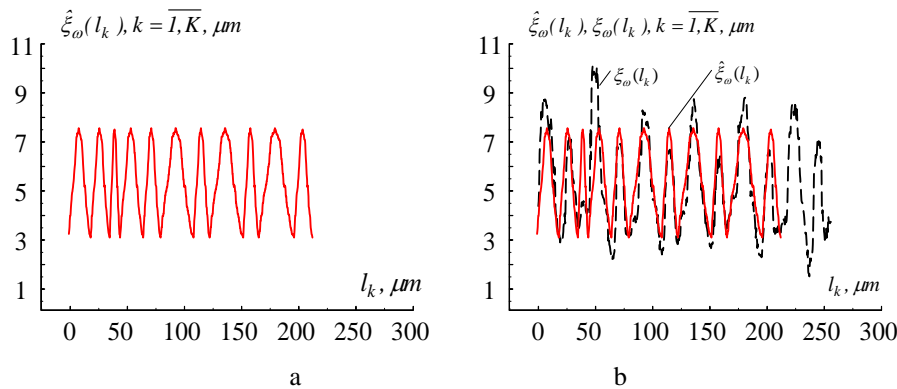


Fig. 6 - The results of computer modeling of the microrelief morphology of titanium alloy Ti6Al4V after exposure to femtosecond laser pulses: a) simulated realization of microrelief; b) experimental and computer simulated realization of microrelief geometry

4. Conclusions

A system of new methods consistent with the mathematical model of methods for identifying the segmental and rhythmic structures of the surface microrelief of titanium alloy Ti6Al4V after exposure to femtosecond laser pulses as part of the stochastic approach is used. The rhythm functions of the studied microrelief are estimated by the method of piecewise linear interpolation. This was possible because single-phase values corresponding to the segments-cycles are considered in the method. The profile diagram of the system of microroughnesses is considered as a diagnostic signal of the surface condition and is described as a cyclic random process. To analyze the microgeometry of the surface relief of the analyzed titanium alloy Ti6Al4V, statistical methods were used and statistical estimates (mathematical expectation and variance) were calculated. This allowed us to expand the apparatus of morphology analysis and computer modeling of microrelief of laser-treated surfaces based on the stochastic approach. In further research, it is planned to modify the mathematical model, which will allow us to consider the features of amplitude values within the structure of the process of forming a laser microrelief for the problem of modeling the surface of metals.

Acknowledgement

The author would like to acknowledge the Ternopil Ivan Puluj National Technical University, 56, Ruska, Ternopil, Ukraine and Microfluidics, Faculty of Mechanical Engineering and Marine Technology, University of Rostock, Justus-von-Liebig-Weg 6, Rostock, Germany.

References

- [1] Wieland, M. (1999) Experimental determination and quantitative evaluation of the surface composition and topography of medical implant surfaces and their influence on osteoblastic cell-surface interactions, Ph.D. thesis no. 13247, 1999, ETH Zürich, Switzerland.
- [2] Schnell, G., Staehlke, S., Duenow, U., Nebe, J.B., Seitz, H. (2019) Femtosecond laser nano/micro textured Ti6Al4V surfaces - effect on wetting and MG-63 cell adhesion. *Materials*, 12, 2210, doi:10.3390/ma12132210.
- [3] Martínez-Calderon, M., Manso-Silvan, M., Rodrıguez, A., Gomez-Aranzadı, M., Garcıa-Ruiz, J. P., Olaizola, S. M., Martın-Palma, R. J., (2016) Surface micro- and nano-texturing of stainless steel by femtosecond laser for the control of cell migration. *Sci Rep* 6, 36296, doi:10.1038/srep36296.
- [4] Shah, F.A., Thomsen, P., and Palmquist, A. (2019) Osteo-integration and current interpretations of the bone-implant interface. *Acta Biomater.* 84, 1-15, doi:10.1016/j.actbio.2018.11.018.
- [5] Lee, B.E.J., Exir, H., Weck, A., Grandfield, K. (2018) Characterization and evaluation of femtosecond laser-induced sub-micron periodic structures generated on titanium to improve osseointegration of implants. *Applied Surface Science* 441,1034-1042, doi:10.1016/j.apsusc.2018.02.119.
- [6] Nosonovsky, M., Bhushan, B. (2008) *Multiscale dissipative mechanisms and hierarchical surfaces: friction, superhydrophobicity, and biomimetics*, Hoboken, NJ: Springer, doi:10.1007/978-3-540-78425-8.
- [7] Cinat, P., Gnecco, G., Paggi, M. (2020) Multi-scale surface roughness optimization through genetic algorithms. *Front. Mech. Eng.*, 2020, doi:10.3389/fmech.2020.00029.
- [8] Gibadullin, I.N., Valetov, V.A. (2017) Automated control of component surface microgeometry using graphic images of the profiles. *Journal of Instrument Engineering*, 60(3), 287-289 (in Russian), doi:10.17586/0021-3454-2017-60-3-287-289
- [9] Bonse, J., Kruger, J., Hohm, S., and Rosenfeld, A. (2012) Femtosecond laser-induced periodic surface structures. *J. Laser Appl.* 24, 042006, doi:10.2351/1.4712658.
- [10] Oliveira, V., Cunha, A., Vilar, R. (2010) Multi-scaled femtosecond laser structuring of stationary titanium surfaces. *Journal of Optoelectronic and Advanced Materials* 12(3), 654-658.
- [11] Konovalov, S., Komissarova, I., Ivanov, Y., Gromov, V., Kosinov, D. (2019) Structural and phase changes under electropulse treatment of fatigue-loaded titanium alloy VT1-0. *Journal of Materials Research and Technology* 8 (1), 1300-1307.
- [12] Ossowska, A., Olive, J.-M., Zielinski, A., Wojtowicz, A. (2021) Effect of double thermal and electrochemical oxidation on titanium alloys for medical applications. *Applied Surface Science*, 563, 150340, doi:10.1016/j.apsusc.2021.150340.
- [13] Lee, C.-H., Choi, S.-W., Narayana, P.L., Nguyen, T.A.N., Hong, S.-T., Kim, J.H., Kang, N., Hong, J.-K. (2021) Effect of electric current heat treatment on commercially pure titanium sheets. *Metals*, 11 (5), 783, doi: 10.3390/met11050783.
- [14] Schnell, G., Duenow, U., Seitz, H. (2020) Effect of laser pulse overlap and scanning line overlap on femtosecond laser-structured Ti6Al4V surfaces. *Materials* 13(4), 969, doi:10.3390/ma13040969.
- [15] Lytvynenko, I., Horkunenko, A., Kuchvara, O., Palaniza, Y. (2019) Methods of processing cyclic signals in automated cardiodiagnostic complexes, *Proceedings of the 1st International Workshop on Information-Communication Technologies & Embedded Systems, (ICT&ES-2019)*, Mykolaiv, November 13-14, 2019, Ukraine, 116-127.
- [16] Chen S.-W., Chen H.-C., Chan H.-L. (2006) A real-time QRS detection method based on moving-averaging incorporating with wavelet denoising. *Computer Methods and Programs in Biomedicine* 82 187-195, doi:10.1016/j.cmpb.2005.11.012.
- [17] Chouhan, V., Mehta, S., Lingayat, N. (2008) Delineation of QRS-complex, P and T-wave in 12-lead ECG. *International Journal of Computer Science and Network Security*, 8, 185-190.
- [18] Israa Shaker Tawfic, Sema Koc Kayhan (2017) Improving recovery of ECG signal with deterministic guarantees using split signal for multiple supports of matching pursuit (SS-MSMP) algorithm. *Computer Methods and Programs in Biomedicine*, 139, 39-50.
- [19] Wartak, J., Milliken J.A., Karchmar J. (1970) Computer program for pattern recognition of electrocardiograms. *Comput. Biomed. Res.*, 3(4), 344-374.
- [20] Pan, J., Tomhins, W. (1985) A real-time QRS detection algorithm. *IEEE Trans. Biomed. Eng.*, 32, 230-236.
- [21] Christov, I. (2004) Real time electrocardiogram QRS detection using combined adaptive threshold. *BioMed. Eng. Online*, 3(28), 9.

- [22] De Chazal, P., Celler, B. (1996) Automatic measurement of the QRS onset and offset in individual ECG leads. *IEEE Engineering in Medicine and Biology Society*, 4, 1399-1403.
- [23] Ebadollah Kheirati Roonizi, Reza Sameni (2013) Morphological modeling of cardiac signals based on signal decomposition, *Computers in Biology and Medicine*, 43(10), 1453-1461.
- [24] Sandeep Raj, Kailash Chandra Ray (2018) Sparse representation of ECG signals for automated recognition of cardiac arrhythmias, *Expert Systems with Applications*, 105, 49-64.
- [25] Santanu Sahoo, Prativa Biswal, Tejaswini Das, Sukanta Sabut. (2016) De-noising of ECG Signal and QRS Detection Using Hilbert Transform and Adaptive Thresholding, *Procedia Technology*, 25, 68-75.
- [26] Lytvynenko, I.V. (2017) The method of segmentation of stochastic cyclic signals for the problems of their processing and modeling. *Journal of Hydrocarbon Power Engineering, Oil and Gas Measurement and Testing*. 4(2), 93-103.
- [27] Lytvynenko, I.V., Maruschak, P.O., Lupenko, S.A., Hats, Yu. I., Menou, A., Panin, S.V. (2016) Software for segmentation, statistical analysis and modeling of surface ordered structures, *AIP Conference Proceedings* 1785, 030012, <https://doi.org/10.1063/1.4967033>.
- [28] Lupenko, S.A. (2007) Zavdannja interpoljacji' funkcii' rytmu cyklichnoi' funkcii' z vidomoju zonnoju strukturoju. *Elektronika ta systemy upravlinnja. Nacional'nyj aviacijnyj universytet*. 2(12), 27-35, (2007). (in Ukrainian)
- [29] Lytvynenko, I.V. (2016) Method of the quadratic interpolation of the discrete rhythm function of the cyclical signal with a defined segment structure. *Scientific Journal of the Ternopil National Technical University*, 84(4), 131-138.